Dynamic Identification of Robots with a Dry Friction Model Depending on Load and Velocity

Pauline Hamon, Maxime Gautier, Philippe Garrec

Dynamic Identification of Robots with a Dry Friction Model Depending on Load and Velocity

P. Hamon[(1)], M. Gautier[(2)], and P. Garrec[(1)]

[(1)] CEA, LIST, Interactive Robotics Laboratory, 18 route du Panorama, BP6, Fontenay-aux-Roses, F-92265, France.
[(2)] University of Nantes/IRCCyN, 1 rue de la Noë, BP 92101, Nantes Cedex 03, F-44321, France.

***Abstract*—Usually, the joint transmission friction model for robots is composed of a viscous friction force and of a constant dry sliding friction force. However, according to the Coulomb law, the dry friction force depends linearly on the load driven by the transmission. It follows that this effect must be taken into account for robots working with large variation of the payload or inertial and gravity forces, and actuated with transmissions as speed reducer, screw-nut or worm gear. This paper proposes a new inverse dynamic identification model for n degrees of freedom (dof) serial robot, where the dry sliding friction force is a linear function of both the dynamic and the external forces, with a velocity-dependent coefficient. A new identification procedure groups all the joint data collected while the robot is tracking planned trajectories with different payloads to get a global least squares estimation of inertial and new friction parameters. An experimental validation is carried out with a joint of an industrial robot.**

I. Introduction

THE usual identification method is based on the inverse dynamic model (IDM) which is linear in relation to the dynamic parameters, and uses least squares (LS) technique. This procedure has been successfully applied to identify inertial and friction parameters of a lot of prototypes and industrial robots [1]-[10]. An approximation of the kinematic Coulomb friction, $F_C sign(\dot{q})$, is widely used to model friction force at non zero velocity $\dot{q}$, assuming that the friction force F_C is a constant parameter. It is identified by moving the robot without any load (or external force) or with constant given payloads [9].

However, the Coulomb law suggests that F_C depends on the transmission force driven in the mechanism. It depends on the dynamic and on the external forces applied through the joint drive chain. Consequently for robots with varying load, the identified IDIM is no more accurate when the transmission uses industrial speed reducer, screw-nut or worm gear because their efficiency significantly varies with the transmitted force. The significant dependence on load has been often observed for transmission elements [15]-[19] through direct measurement procedures. Moreover, the mechanism efficiency depends on the sense of power transfer leading to two distinct sets of friction parameters. In addition, when the robot moves at very low velocity, as for teleoperation, one observes a velocity-dependency of the dry friction.

This paper presents a new inverse dynamic identification model for n degrees of freedom (dof) serial robot, where the dry sliding friction force F_C is a linear function of both the dynamic and the external forces, with asymmetrical behavior depending on the signs of joint force and velocity, and a variation depending on the velocity amplitude. A new identification procedure is proposed. All the joint position and joint force data collected in several experiments, while the robot is tracking planned trajectories with different payloads, are concatenated to calculate a global least squares estimation of both the inertial and the new friction parameters.

An experimental validation is carried out on the third joint of an industrial robot: Stäubli RX130L [25]. Both models are compared.

II. Usual Inverse Dynamic Modeling and Identification

A. Modeling

In the following, all mechanical variables are given in SI units in the joint space. All forces, positions, velocities and accelerations have a conventional positive sign in the same direction. That defines a motor convention for the mechanical behavior.

The dynamic model of a rigid robot composed of n moving links is written as follows [11]:

$$\boldsymbol{\tau}_{dyn} = \boldsymbol{\tau}_{in} + \boldsymbol{\tau}_{f} + \boldsymbol{\tau}_{ext} \tag{1}$$

where:

- $\boldsymbol{\tau}_{dyn}$ is the (nx1) vector of dynamic forces due to the inertial, centrifugal, Coriolis, and gravitational effects:

$$\boldsymbol{\tau}_{dyn} = \boldsymbol{M}(\boldsymbol{q})\ddot{\boldsymbol{q}} + \boldsymbol{C}(\boldsymbol{q},\dot{\boldsymbol{q}})\dot{\boldsymbol{q}} + \boldsymbol{Q}(\boldsymbol{q}) \tag{2}$$

where $\boldsymbol{q}$, $\dot{\boldsymbol{q}}$ and $\ddot{\boldsymbol{q}}$ are respectively the (nx1) vectors of generalized joint positions, velocities and accelerations, $\boldsymbol{M}(\boldsymbol{q})$ is the (nxn) robot inertia matrix, $\boldsymbol{C}(\boldsymbol{q}, \dot{\boldsymbol{q}})$ is the (nxn) matrix of centrifugal and Coriolis effects, $\boldsymbol{Q}(\boldsymbol{q})$ is the (nx1) vector of gravitational forces.

- $\boldsymbol{\tau}_{in}$ is the (nx1) input torque vector on the motor side of the drive chain:

$$\boldsymbol{\tau}_{in} = \boldsymbol{g}_f (\boldsymbol{v}_f - \boldsymbol{v}_{f_0}) \quad (3)$$

where $\boldsymbol{v}_f$ is the (nx1) vector of current references of the current amplifiers, $\boldsymbol{v}_{f_0}$ is a (nx1) vector of amplifiers offsets, $\boldsymbol{g}_f$ is the (nxn) matrix of the drive gains,

$$\boldsymbol{g}_f = \boldsymbol{N}\boldsymbol{G}_i\boldsymbol{K}_t \quad (4)$$

$\boldsymbol{N}$ is the (nxn) gear ratios matrix of the joint drive chains ($\dot{\boldsymbol{q}}_{\mathrm{m}} = \boldsymbol{N}\dot{\boldsymbol{q}}$ with $\dot{\boldsymbol{q}}_{\mathrm{m}}$ the (nx1) velocities vector on the motor side), $\boldsymbol{G}_i$ is the (nxn) static gains diagonal matrix of the current amplifiers, $\boldsymbol{K}_t$ is the (nxn) diagonal matrix of the electromagnetic motor torque constants [14].

- $\boldsymbol{\tau}_f$ is the (nx1) vector of the loss force due to frictions. Usually, it is approximated with a viscous friction and a dry friction:

$$\boldsymbol{\tau}_f = -\boldsymbol{F}_V\dot{\boldsymbol{q}} - \boldsymbol{F}_C\boldsymbol{sign}(\dot{\boldsymbol{q}}) - \boldsymbol{F}_{Coff} \quad (5)$$

where $\boldsymbol{F}_V$ is the (nxn) diagonal matrix of viscous parameters, $\boldsymbol{F}_C$ is the (nxn) diagonal matrix of dry friction parameters, and $\boldsymbol{sign}(.)$ denotes the sign function, $\boldsymbol{F}_{Coff}$ is a (nx1) vector of asymmetrical Coulomb friction force between positive and negative velocities. This friction model is linear to $\boldsymbol{F}_V$ and $\boldsymbol{F}_C$ (Fig. 1.a).

- $\boldsymbol{\tau}_{ext}$ is the (nx1) external forces vector in the joint space.

Thus (1) becomes:

$$\begin{aligned} \boldsymbol{\tau}_{dyn} - \boldsymbol{\tau}_{ext} &= \boldsymbol{g}_f\boldsymbol{v}_f - \boldsymbol{F}_V\dot{\boldsymbol{q}} - \boldsymbol{F}_C\boldsymbol{sign}(\dot{\boldsymbol{q}}) - (\boldsymbol{F}_{Coff} + \boldsymbol{g}_f\boldsymbol{v}_{f_0}) \\ \Leftrightarrow \quad \boldsymbol{\tau}_{out} &= \boldsymbol{\tau} - \boldsymbol{F}_V\dot{\boldsymbol{q}} - \boldsymbol{F}_C\boldsymbol{sign}(\dot{\boldsymbol{q}}) - \boldsymbol{\tau}_{off} \end{aligned} \quad (6)$$

where $\boldsymbol{\tau}_{out} = \boldsymbol{\tau}_{dyn} - \boldsymbol{\tau}_{ext}$ is the output force (the load force) of the drive chain, $\boldsymbol{\tau}_{off} = \boldsymbol{F}_{Coff} + \boldsymbol{g}_f\boldsymbol{v}_{f_0}$ is an offset force that regroups the amplifier offset and the asymmetrical Coulomb friction coefficient.

$$\boldsymbol{\tau} = \boldsymbol{g}_f\boldsymbol{v}_f \quad (7)$$

is the motor force, without offset, and defined by $\boldsymbol{v}_f$ which is the current reference calculated by the numerical control and stored for the identification.

Then (1) can be rewritten as the inverse dynamic model (IDM) which calculates the motor torque vector $\boldsymbol{\tau}$ as a function of the generalized coordinates:

$$\begin{aligned} \boldsymbol{\tau} &= \boldsymbol{M}(\boldsymbol{q})\ddot{\boldsymbol{q}} + \boldsymbol{C}(\boldsymbol{q},\dot{\boldsymbol{q}})\dot{\boldsymbol{q}} + \boldsymbol{Q}(\boldsymbol{q}) + \boldsymbol{F}_C\boldsymbol{sign}(\dot{\boldsymbol{q}}) + \boldsymbol{F}_V\dot{\boldsymbol{q}} + \boldsymbol{\tau}_{off} - \boldsymbol{\tau}_{ext} \\ &= \boldsymbol{\tau}_{out} + \boldsymbol{F}_C\boldsymbol{sign}(\dot{\boldsymbol{q}}) + \boldsymbol{F}_V\dot{\boldsymbol{q}} + \boldsymbol{\tau}_{off} \end{aligned} \quad (8)$$

B. Identification

The choice of the modified Denavit and Hartenberg frames attached to each link allows to obtain a dynamic model linear in relation to a set of standard dynamic parameters $\boldsymbol{\chi}_{St}$ [6], [11]:

$$\boldsymbol{\tau} = \boldsymbol{D}_{St}(\boldsymbol{q},\dot{\boldsymbol{q}},\ddot{\boldsymbol{q}})\boldsymbol{\chi}_{St} \quad (9)$$

where $\boldsymbol{D}_{St}(\boldsymbol{q},\dot{\boldsymbol{q}},\ddot{\boldsymbol{q}})$ is the regressor and $\boldsymbol{\chi}_{St}$ is the vector of the standard parameters which are the coefficients XX_j, XY_j, XZ_j, YY_j, YZ_j, ZZ_j of the inertia tensor of link j denoted ${}^j\boldsymbol{J}_j$, the mass of the link j called m_j, the first moments vector of link j around the origin of frame j denoted ${}^j\boldsymbol{M}_j = [MX_j\ MY_j\ MZ_j]^{\mathrm{T}}$, the friction coefficients F_{Vj}, F_{Cj}, the actuator inertia called Ia_j, and the offset $\tau_{off\,j}$. The velocities and accelerations are calculated using well tuned band pass filtering of the joint position [7].

The base parameters are the minimum number of parameters from which the dynamic model can be calculated. They are obtained by eliminating and by regrouping some standard inertial parameters [12], [13]. The minimal inverse dynamic model can be written as:

$$\boldsymbol{\tau} = \boldsymbol{D}(\boldsymbol{q},\dot{\boldsymbol{q}},\ddot{\boldsymbol{q}})\boldsymbol{\chi} \quad (10)$$

where $\boldsymbol{D}(\boldsymbol{q},\dot{\boldsymbol{q}},\ddot{\boldsymbol{q}})$ is the minimal regressor and $\boldsymbol{\chi}$ is the vector of the base parameters.

The inverse dynamic model (10) is sampled while the robot is tracking a trajectory to get an over-determined linear system such that [6]:

$$\boldsymbol{Y}(\boldsymbol{\tau}) = \boldsymbol{W}(\boldsymbol{q},\dot{\boldsymbol{q}},\ddot{\boldsymbol{q}})\boldsymbol{\chi} + \boldsymbol{\rho} \quad (11)$$

with $\boldsymbol{Y}(\boldsymbol{\tau})$ the measurements vector, $\mathbf{W}$ the observation matrix and $\boldsymbol{\rho}$ the vector of errors.

The LS solution $\hat{\boldsymbol{\chi}}$ minimizes the 2-norm of the vector of errors $\boldsymbol{\rho}$. $\boldsymbol{W}$ is a (r×b) full rank and well conditioned matrix where $\mathrm{r} = \mathrm{N_e}\,\mathrm{x}\,\mathrm{n}$, with $\mathrm{N_e}$ the number of samples on the trajectories. The LS solution $\hat{\boldsymbol{\chi}}$ is given by:

$$\hat{\boldsymbol{\chi}} = \left(\boldsymbol{W}^{\mathrm{T}}\boldsymbol{W}\right)^{-1}\boldsymbol{W}^{\mathrm{T}}\boldsymbol{Y} = \boldsymbol{W}^{+}\boldsymbol{Y} \quad (12)$$

It is calculated using the QR factorization of $\boldsymbol{W}$. Standard deviations $\boldsymbol{\sigma}_{\hat{\chi}_i}$ are estimated using classical and simple results from statistics. The matrix $\boldsymbol{W}$ is supposed to be deterministic, and $\boldsymbol{\rho}$, a zero-mean additive independent noise, with a standard deviation such as:

$$\boldsymbol{C}_{\rho\rho} = \mathrm{E}\left(\boldsymbol{\rho}\boldsymbol{\rho}^{\mathrm{T}}\right) = \sigma_\rho^2\boldsymbol{I}_r \quad (13)$$

where E is the expectation operator and $\boldsymbol{I}_r$, the (r×r) identity matrix. An unbiased estimation of σ_ρ is:

$$\hat{\sigma}_\rho^2 = \left\|\boldsymbol{Y} - \boldsymbol{W}\hat{\boldsymbol{\chi}}\right\|^2 \Big/ (r-b) \quad (14)$$

The covariance matrix of the standard deviation is calculated as follows:

$$\boldsymbol{C}_{\hat{\chi}\hat{\chi}} = \mathrm{E}\left[(\boldsymbol{\chi} - \hat{\boldsymbol{\chi}})(\boldsymbol{\chi} - \hat{\boldsymbol{\chi}})^{\mathrm{T}}\right] = \sigma_\rho^2(\boldsymbol{W}^{\mathrm{T}}\boldsymbol{W})^{-1} \quad (15)$$

$\sigma_{\hat{\chi}_i}^2 = C_{\hat{\chi}\hat{\chi}ii}$ is the i$^{\mathrm{th}}$ diagonal coefficient of $\boldsymbol{C}_{\hat{\chi}\hat{\chi}}$. The

relative standard deviation $\%\sigma_{\hat{\chi}_{ri}}$ is given by:

$$\%\sigma_{\hat{\chi}_{ri}} = 100\,\sigma_{\hat{\chi}_i} / \hat{\chi}_i \tag{16}$$

However, experimental data are corrupted by noise and error modeling and $\boldsymbol{W}$ is not deterministic. This problem can be solved by filtering the measurement vector $\boldsymbol{Y}$ and the columns of the observation matrix $\boldsymbol{W}$ as described in [7], [8].

III. New Dry Friction Model and Identification

In this section, we introduce a dry friction model dependent on the load, that is $\boldsymbol{\tau}_{out}$, and on the velocity $\dot{\boldsymbol{q}}$.

A. Load-Dependent Friction Model

The Coulomb friction is still written $\boldsymbol{F}_C sign(\dot{\boldsymbol{q}})$, with $\boldsymbol{F}_C$ a (nxn) diagonal matrix. But here, for each link *j*, $\boldsymbol{F}_{C(j,j)}$ (the $(j,j)^{th}$ element of the matrix $\boldsymbol{F}_C$) depends linearly on the absolute value of the load of joint *j* which is $\tau_{out\,j}$ (Fig. 1.b), [15]-[19]. As one can see in II.B, $\tau_{out\,j}$ is a function of $\boldsymbol{q}, \dot{\boldsymbol{q}}, \ddot{\boldsymbol{q}}$ and is linear in relation to base parameters.

Then the inverse dynamic model for each link *j* becomes:

$$\tau_j = \tau_{out\,j} + \left(\alpha_j \left|\tau_{out\,j}\right| + \beta_j\right) sign(\dot{q}_j) + \boldsymbol{F}_{V(j,j)}\dot{q}_j + \tau_{off\,j} \tag{17}$$

where α_j and β_j are parameters to be identified. These new parameters depend on the mechanical structure of the reducers used to actuate the robot.

For ease of understanding, the subscript *j* is omitted for all variables in the following to simplify the notation.

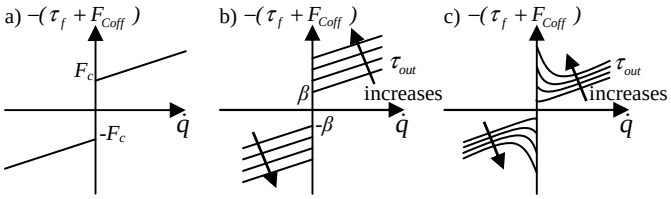

Fig. 1. a) Usual friction model with constant dry friction + viscous friction.
b) Model with load-dependent dry friction + viscous friction.
c) Model with load- and velocity-dependent dry friction + viscous friction.

The inverse dynamic model can be written as follows:

$$\tau = \tau_{out} + \alpha\left|\tau_{out}\right| sign(\dot{q}) + \beta sign(\dot{q}) + F_V\dot{q} + \tau_{off} \tag{18}$$

And with $\left|\tau_{out}\right| = \tau_{out} sign(\tau_{out})$ and
$sign(\tau_{out})sign(\dot{q}) = sign(\tau_{out}\dot{q}) = sign(P_{out})$, one obtains:

$$\tau = \tau_{out} + \alpha\tau_{out} sign(P_{out}) + \beta sign(\dot{q}) + F_V\dot{q} + \tau_{off} \tag{19}$$

Thus, the IDM depends on the signs of the output power $P_{out} = \tau_{out}\dot{q}$. One defines 4 quadrants in the frame $(\dot{q}, \tau_{out})$, which can be grouped two by two (Fig. 2.a). In the quadrants 1 and 3, P_{out} is positive and the actuator has a motor behavior. In the quadrants 2 and 4, P_{out} is negative and the actuator has a generator behavior which may save the power to the power supply, assuming a 4 quadrants amplifier.

B. Dry Friction Model Depending on the Power Sign

In the model (19), α and β do not depend on the output power sign. But, generally they take different values: α_m and β_m for the motor quadrants, and α_g and β_g for the generator quadrants.

$$\begin{cases} P_{out} > 0 \Rightarrow \tau = (1+\alpha_m)\tau_{out} + \beta_m sign(\dot{q}) + F_V\dot{q} + \tau_{off} \\ P_{out} < 0 \Rightarrow \tau = (1-\alpha_g)\tau_{out} + \beta_g sign(\dot{q}) + F_V\dot{q} + \tau_{off} \end{cases} \tag{20}$$

The model (20) is illustrated in Fig. 2.b for a constant velocity $\left|\dot{q}_0\right|$. This model is not valid anymore for very low forces in the stiction area ($\dot{q} = 0$): one approximates the friction as the limit of model (20) in the rectangle $\left(\beta_m + F_V\left|\dot{q}_0\right| + \tau_{off}\ ;\ (\beta_g + F_V\left|\dot{q}_0\right| - \tau_{off})/(1-\alpha_g)\right)$.

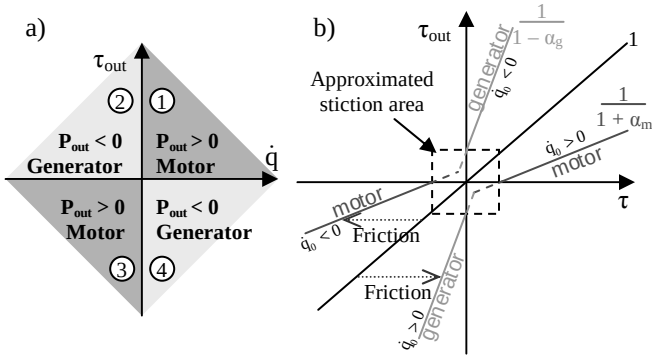

Fig. 2. a) Four quadrants frame $(\dot{q}, \tau_{out})$ for motor or generator behavior.
b) Asymmetrical friction for a given velocity $\dot{q}_0$ and the stiction area.

C. Dry Friction Model Depending on the Velocity

For a robot moving at low velocities, one observes a dry friction variation, functions of the velocity, which is similar to the Stribeck model (Fig. 1.c), [20], [21], [22].

$$F = \begin{cases} \tau_{out} & \text{if } \dot{q} = 0 \text{ and } \left|\tau_{out}\right| < F_{st} \\ F_{st} sign(\tau_{out}) & \text{if } \dot{q} = 0 \text{ and } \left|\tau_{out}\right| \geq F_{st} \\ F(\dot{q}) & \text{if } \dot{q} \neq 0 \end{cases} \tag{21}$$

with:

$$F(\dot{q}) = \left(F_{sl} + (F_{st} - F_{sl})e^{-\left|\dot{q}/\dot{q}_s\right|}\right) sign(\dot{q}) \tag{22}$$

where $\dot{q}_S$ is a velocity constant, F_{st} is the dry friction in stiction and F_{sl} is the dry friction in sliding mode.

To combine the variation due to the load (17) with the one due to velocity (22), one takes:

$$F_{sl} = \alpha\left|\tau_{out}\right| + \beta \text{ et } F_{st} = \gamma\left|\tau_{out}\right| + \delta \tag{23}$$

Then, (22) becomes:

$$F(\dot{q}) = \left(\alpha|\tau_{out}| + \beta + (\gamma|\tau_{out}| + \delta - \alpha|\tau_{out}| - \beta)e^{-|\dot{q}|/\dot{q}_S}\right) sign(\dot{q})$$
$$= \left(\alpha + (\gamma - \alpha)e^{-|\dot{q}|/\dot{q}_S}\right)\tau_{out}\, sign(P_{out}) + \left(\beta + (\delta - \beta)e^{-|\dot{q}|/\dot{q}_S}\right) sign(\dot{q}) \quad (24)$$

Because of the dependence on power sign, one has 2 sets of parameters α, β, γ, δ for the 2 behaviors: motor and generator. Considering $a_m = 1 + \alpha_m$, $b_m = \gamma_m - \alpha_m$, $c_m = \beta_m$, $d_m = \delta_m - \beta_m$, and $a_g = 1 - \alpha_g$, $b_g = \gamma_g - \alpha_g$, $c_g = \beta_g$, $d_g = \delta_g - \beta_g$, the inverse dynamic model becomes:

$$\begin{cases} \bullet\, P_{out} > 0 \;\Rightarrow \\ \quad \tau = a_m\tau_{out} + b_m\tau_{out}e^{-|\dot{q}|/\dot{q}_S} + c_m sign(\dot{q}) + d_m e^{-|\dot{q}|/\dot{q}_S} sign(\dot{q}) + F_V\dot{q} + \tau_{off} \\ \bullet\, P_{out} < 0 \;\Rightarrow \\ \quad \tau = a_g\tau_{out} - b_g\tau_{out}e^{-|\dot{q}|/\dot{q}_S} + c_g sign(\dot{q}) + d_g e^{-|\dot{q}|/\dot{q}_S} sign(\dot{q}) + F_V\dot{q} + \tau_{off} \end{cases} \quad (25)$$

D. Friction Identification Method

In order to keep a IDM linear in relation to the parameters, one decides on an a priori value of $\dot{q}_S$. This constant represents the exponential transitional behavior between stiction and sliding, that is about $3 * \dot{q}_S$, more or less 5%. Measurements show that the amplitude of this transitional behavior is close to 10% of the nominal velocity 1.2 rad/s, that is $\dot{q}_S = 0.04$ rad/s. A final adjustment to $\dot{q}_S = 0.03$ rad/s at the moment of the identification gives a minimal residual $\|\rho\|$ a little lower. This value for $\dot{q}_S$ is close to the value given in [22] for a Kuka IR 161 robot.

Furthermore, the model (25) depends on the sign of P_{out} which is unknown. To overcome this problem, the samples of τ measurements are selected outside of the stiction area ($\dot{q} = 0$ – Fig. 2.b) in order to get the same sign for τ_{out} and τ. This allows to get the sign of P_{out} with:

$$sign(P_{out}) = sign(\tau_{out}\dot{q}) = sign(\tau\dot{q}) = sign(P) \quad (26)$$

One can then write the IDM linear in relation to parameters and use the LS technique. To have only one expression instead of two in (25), 3 variables are introduced, P^+, P^-, and E_{xp}, defined by:

$$P^+ = \frac{1 + sign(P)}{2},\ P > 0 \Leftrightarrow P^+ = 1,\ P < 0 \Leftrightarrow P^+ = 0 \quad (27)$$

$$P^- = \frac{1 - sign(P)}{2} = \bar{P}^+ \quad (28)$$

$$E_{xp} = e^{-|\dot{q}|/\dot{q}_S} \quad (29)$$

The inverse dynamic model is then written:

$$\tau = P^+(a_m + b_m E_{xp})\tau_{out} + P^-(a_g - b_g E_{xp})\tau_{out} + \ldots$$
$$\ldots P^+(c_m + d_m E_{xp})sign(\dot{q}) + P^-(c_g + d_g E_{xp})sign(\dot{q}) + F_V\dot{q} + \tau_{off} \quad (30)$$

As τ_{out} is linear in relation to parameters, so is τ.

IV. Experimental Setup and Identification

A. Study case: Stäubli RX130L Robot

The Stäubli RX130L robot is an industrial robot with 6 rotational joints. The joint 3 has been chosen for this study because unlike the joint 1, it has large gravity variation, and no compensation gravity spring contrary to the joint 2. The links 1 and 2 are lined up and locked in a vertical position. The arm 3 is composed of the links 4, 5 and 6 brought into line with the link 3 and locked (Fig. 3), with a total mass of about 30 kg and a length of 1.33 m. The maximum velocity is 1.2 rad/s and the maximum acceptable load at the extremity is 10 kg.

The inverse dynamic model of joint 3 is written:

$$\tau_3 = J_3\ddot{q}_3 + MX_3 g\cos(q_3) + MY_3 g\sin(q_3) + F_{C3}sign(\dot{q}_3) + F_{V3}\dot{q}_3 + \tau_{off3} \quad (31)$$

where:

- $J_3 = Ia_3 + ZZ_3$ is the inertia moment Ia_3 of the drive chain plus the inertia moment ZZ_3 of the arm,
- $g = 9.81$ m/s^2 is the gravity acceleration.

All variables and parameters are given in SI units on the joint space. In the following, the subscript 3 is omitted to simplify the notation.

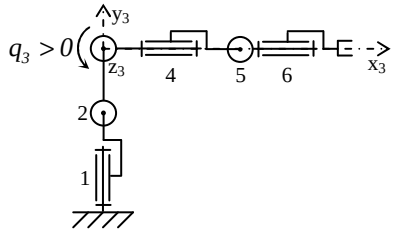

Fig. 3. RX130L drawing: joints 1, 2, 4, 5 and 6 locked in position.

B. Data Acquisition

The identification of dynamic parameters is carried out with and without payloads: two different additional masses can be fixed to the arm extremity. To excite properly the friction parameters to be identified, sinusoidal and trapezoidal velocities trajectories were used.

The estimation of $\dot{q}$ and $\ddot{q}$ are carried out with pass band filtering of q consisting of a low pass Butterworth filter and a central derivative algorithm. The Matlab function *filtfilt* can be used [23]. The motor torque is calculated using the current reference (7). In order to cancel high frequency ripple in τ, the vector $\boldsymbol{Y}$ and the columns of the observation matrix $\boldsymbol{W}$ are both low pass filtered and decimated. This parallel filtering procedure is carried out with the Matlab *decimate* function [2], [10].

C. Identification

To identify the load-dependent friction, measurements

with known payloads are used. Gravity and inertial forces due to the additional mass fixed to the robot extremity have to be added in the IDM.

Let R_m be the frame set at the center of gravity G_m of the additional masse M_a, and parallel to the frame $R_3(x_3, y_3, z_3)$ linked to the arm (Fig. 3). One gives the inertia matrix I_{Ga} of the additional mass which is a disk with a radius r and a thickness l:

$$I_{Ga} = \begin{bmatrix} M_a r^2/2 & 0 & 0 \\ 0 & M_a(r^2/4 + l^2/12) & 0 \\ 0 & 0 & M_a(r^2/4 + l^2/12) \end{bmatrix}_{(G_m, R_m)} \quad (32)$$

The vector of translation between R_3 and R_m is $T = \begin{bmatrix} L_a & 0 & 0 \end{bmatrix}^{\mathrm{T}}$ and as the 2 frames are parallel, one can apply the Huygens theorem:

$$J_a = \begin{bmatrix} M_a r^2/2 & 0 & 0 \\ 0 & M_a(r^2/4 + l^2/12) & 0 \\ 0 & 0 & M_a(r^2/4 + l^2/12) + M_a L_a^2 \end{bmatrix} \quad (33)$$

As the terms r^2 and e^2 are negligible, compared with L_a^2, one keeps only the term $M_a L_a^2 \ddot{q}$.

For the gravity, considering the vector of translation T, one has: $M_a L_a g \cos(q)$.

Thus, for the samples $\tau_{(k)}$ with an additional mass $M_{a(k)}$, (31) becomes:

$$\begin{aligned} \tau_{(k)} = {} & J\ddot{q} + MXg\cos(q) + MYg\sin(q) + M_{a(k)} L_a^2 \ddot{q} + \dots \\ & \dots M_{a(k)} L_a g \cos(q) + F_C \operatorname{sign}(\dot{q}) + F_V \dot{q} + \tau_{off} \end{aligned} \quad (34)$$

where:

- $M_{a(k)}$ is one of the additional masses, fixed to robot extremity, with accurate weighed values: 0 kg, 3.4584 kg and 6.970 kg,
- L_a is the length from the joint 3 to the additional mass position (measured distance): 1.277 m

At a first step, to identify the usual model with all samples, one distinguishes the weighed mass M_{aw} and the mass M_{ae} estimated by the identification. Thus, the usual model is:

$$\begin{aligned} \tau_{(k)} = {} & J\ddot{q} + MXg\cos(q) + MYg\sin(q) + \dots \\ & \dots \frac{M_{ae(k)}}{M_{aw(k)}} M_{aw(k)} L_a (L_a \ddot{q} + g\cos(q)) + F_C \operatorname{sign}(\dot{q}) + F_V \dot{q} + \tau_{off} \end{aligned} \quad (35)$$

Then, the sampled measurements, for k from 1 to 3, are concatenated using the $M_{aw(k)}$ corresponding to each experiment (k), to get the linear system:

$$\boldsymbol{Y}_{\text{usual}} = \boldsymbol{W}_{\text{usual}} \boldsymbol{\chi}_{\text{usual}} + \boldsymbol{\rho}_{\text{usual}} \quad (36)$$

with the measurements vector, the observation matrix, and the vector of base parameters below:

$$\boldsymbol{Y}_{\text{usual}} = \boldsymbol{\tau} = \begin{bmatrix} \boldsymbol{\tau}_{(1)}^{\mathrm{T}} & \boldsymbol{\tau}_{(2)}^{\mathrm{T}} & \boldsymbol{\tau}_{(3)}^{\mathrm{T}} \end{bmatrix}^{\mathrm{T}} \quad (37)$$

$$\boldsymbol{W}_{usual} = \begin{bmatrix} \ddot{\boldsymbol{q}} & g\cos(\boldsymbol{q}) & g\sin(\boldsymbol{q}) & M_{aw} L_a (L_a \ddot{\boldsymbol{q}} + g\cos(\boldsymbol{q})) & \operatorname{sign}(\dot{\boldsymbol{q}}) & \dot{\boldsymbol{q}} & \boldsymbol{1} \end{bmatrix} \quad (38)$$

$$\boldsymbol{\chi}_{usual} = \begin{bmatrix} J & MX & MY & \dfrac{M_{ae}}{M_{aw}} & F_C & F_V & \tau_{off} \end{bmatrix}^{\mathrm{T}} \quad (39)$$

At a second step, the proposed model is identified with:

$$\boldsymbol{Y}_{\text{new}} = \boldsymbol{W}_{\text{new}} \boldsymbol{\chi}_{\text{new}} + \boldsymbol{\rho}_{\text{new}} \quad (40)$$

with the measurements vector, the observation matrix, and the vector of base parameters defined as follows:

$$\boldsymbol{Y}_{\text{new}} = \boldsymbol{Y}_{\text{usual}} = \boldsymbol{\tau} \quad (41)$$

$$\begin{aligned} \boldsymbol{W}_{new} = \Big[& \boldsymbol{P}^+ \ddot{\boldsymbol{q}} \quad \boldsymbol{P}^+ \boldsymbol{E}_{xp} \ddot{\boldsymbol{q}} \quad \boldsymbol{P}^+ g\cos(\boldsymbol{q}) \quad \dots \\ & \dots \quad \boldsymbol{P}^+ \boldsymbol{E}_{xp} g\cos(\boldsymbol{q}) \quad \boldsymbol{P}^+ g\sin(\boldsymbol{q}) \quad \boldsymbol{P}^+ \boldsymbol{E}_{xp} g\sin(\boldsymbol{q}) \quad \dots \\ & \dots \quad \boldsymbol{P}^+ M_a L_a (L_a \ddot{\boldsymbol{q}} + g\cos(\boldsymbol{q})) \quad \boldsymbol{P}^+ \boldsymbol{E}_{xp} M_a L_a (L_a \ddot{\boldsymbol{q}} + g\cos(\boldsymbol{q})) \quad \dots \\ & \dots \quad \boldsymbol{P}^- \ddot{\boldsymbol{q}} \quad -\boldsymbol{P}^- \boldsymbol{E}_{xp} \ddot{\boldsymbol{q}} \quad \boldsymbol{P}^- g\cos(\boldsymbol{q}) \quad \dots \\ & \dots \quad -\boldsymbol{P}^- \boldsymbol{E}_{xp} g\cos(\boldsymbol{q}) \quad \boldsymbol{P}^- g\sin(\boldsymbol{q}) \quad -\boldsymbol{P}^- \boldsymbol{E}_{xp} g\sin(\boldsymbol{q}) \quad \dots \\ & \dots \quad \boldsymbol{P}^- M_a L_a (L_a \ddot{\boldsymbol{q}} + g\cos(\boldsymbol{q})) \quad -\boldsymbol{P}^- \boldsymbol{E}_{xp} M_a L_a (L_a \ddot{\boldsymbol{q}} + g\cos(\boldsymbol{q})) \quad \dots \\ & \dots \quad \boldsymbol{P}^+ \operatorname{sign}(\dot{\boldsymbol{q}}) \quad \boldsymbol{P}^+ \boldsymbol{E}_{xp} \operatorname{sign}(\dot{\boldsymbol{q}}) \quad \boldsymbol{P}^- \operatorname{sign}(\dot{\boldsymbol{q}}) \quad \boldsymbol{P}^- \boldsymbol{E}_{xp} \operatorname{sign}(\dot{\boldsymbol{q}}) \quad \dot{\boldsymbol{q}} \quad \boldsymbol{1} \Big] \end{aligned}$$

$$\begin{aligned} \boldsymbol{\chi}_{new} = \Big[& a_m J \quad b_m J \quad a_m MX \quad b_m MX \quad a_m MY \quad b_m MY \quad a_m \quad b_m \quad \dots \\ & \dots \quad a_g J \quad b_g J \quad a_g MX \quad b_g MX \quad a_g MY \quad b_g MY \quad a_g \quad b_g \quad \dots \\ & \dots \quad c_m \quad d_m \quad c_g \quad d_g \quad F_V \quad \tau_{off} \Big]^{\mathrm{T}} \end{aligned} \quad (43)$$

The expressions of $\boldsymbol{W}_{\text{new}}$ and $\boldsymbol{\chi}_{\text{new}}$ are obtained by inserting $\tau_{out} = J\ddot{q} + MXg\cos(q) + MYg\sin(q) + M_a L_a (L_a \ddot{q} + M_a g\cos(q))$ in the inverse dynamic model (30).

Here $\boldsymbol{P}^+$, $\boldsymbol{P}^-$, and $\boldsymbol{E}_{xp}$ are diagonal matrices, with:

$$\boldsymbol{P}_{i,i}^+ = \frac{1 + \operatorname{sign}(\boldsymbol{P}_i)}{2}, \quad \boldsymbol{P}_{i,i}^- = \frac{1 - \operatorname{sign}(\boldsymbol{P}_i)}{2}, \quad \boldsymbol{E}_{xp(i,i)} = e^{-|\dot{q}_i|/\dot{q}_s} \quad (44)$$

The two models are compared using exactly the same identification method with the same measurements.

D. Results

The significant values identified with usual IDM and OLS regressions are given in Table I and those with the new IDM in Table II (the parameters with a large relative deviation are not significant and have been eliminated). For each model, Fig. 4 and Fig. 5 present a direct validation comparing the actual $\boldsymbol{\tau}$ with its predicted value $\boldsymbol{W}\hat{\boldsymbol{\chi}}$. Moreover, Table III

presents the relative norm of errors $\|\boldsymbol{\rho}\|/\|\boldsymbol{Y}\|$ for the two models and for several sets of experiments: all measurements (all velocities), with low velocities (0 to 10% of the maximum velocity) or high velocities (35% to 100% of the maximum velocity). Finally, Table IV compares the relative norms of errors for the two models, with two different identifications: the first one is carried out with all measurements, that is with variation of the payload fixed to arm extremity, and the second one is carried out with only the samples obtained without payload.

As one can see in all figures and tables, the new dynamic model improves the residual.

TABLE I
IDENTIFIED VALUES WITH USUAL IDM

Parameters	Identified Values	Standard deviation * 2	Relative deviation
J	30.921	0.283	0.46 %
MX	21.109	0.016	0.04 %
M_{ae}/M_{ap}	0.922	0.003	0.15 %
F_C	39.890	0.084	0.11 %
F_V	29.429	0.395	0.67 %
τ_{off}	9.931	0.077	0.39 %

TABLE II
IDENTIFIED VALUES WITH NEW IDM

Parameters	Identified Values	Standard deviation * 2	Relative deviation
a_mJ	32.420	0.262	0.40 %
a_mMX	22.204	0.033	0.07 %
b_mMX	1.621	0.050	1.55 %
a_m	0.942	0.005	0.25 %
b_m	0.240	0.008	1.72 %
a_qJ	29.294	0.276	0.47 %
a_qMX	19.432	0.042	0.11 %
b_qMX	1.798	0.051	1.43 %
a_q	0.915	0.005	0.27 %
b_q	0.266	0.008	1.59 %
c_m	21.152	0.143	0.34 %
c_q	15.588	0.244	0.78 %
F_V	48.139	0.317	0.33 %
τ_{off}	9.950	0.051	0.26 %

TABLE III
RELATIVE NORM OF ERRORS WITH BOTH MODELS

Measurements used	Usual model	New model
All Samples (all velocities)	0.0733	0.0484
Samples with low velocities	0.0737	0.0401
Samples with high velocities	0.0863	0.0881

TABLE IV
RELATIVE NORM OF ERRORS FOR 2 IDENTIFICATIONS

Identification carried out	Usual model	New model
With payload variations	0.0733	0.0484
Without payload	0.0742	0.0598

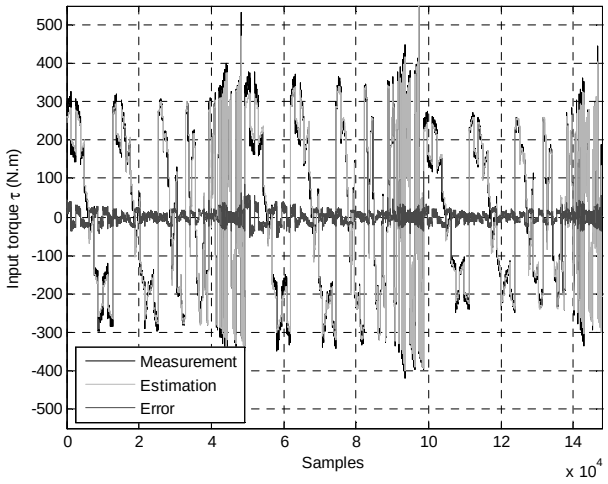

Fig. 4. Direct validation performed with usual IDM.

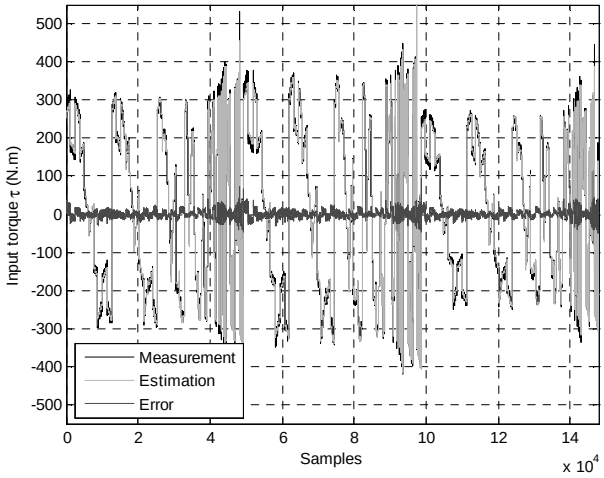

Fig. 5. Direct validation performed with new IDM.

V. DISCUSSION

The parameters of the new model are identifiable (low standard deviation) and so significant. The identification process does not change as the new model is still linear in relation to the parameters. The originality is that the global identification groups all measurements, with all payloads, in only one LS process. The main difficulty is to distinguish the different behaviours, motor and generator, but a solution has been proposed along this paper. One can also note that the measurements have to be more exciting than usual: each test has to be done with different loads and low velocities to highlight the effect on the friction variations. So, this identification protocol is more time-consuming and the setting up must be adapted for the measurements with additional masses.

The figures of direct validation show an improvement of the estimated torque by the new model, which is confirmed by the Table III. Indeed, one observes a decrease of 34% in the relative norm of errors. The improvement is mostly important for the low velocities where the errors are divided

by two, thanks to the new model (decrease of 46%). At high velocity, the friction term with the exponential function approaches zero, and the new model is equivalent to the usual.

Moreover, the Table IV shows that the model is especially interesting for robots carrying some payloads. However, for a robot without payload but with high gravity variation, as the third joint of the RX130L, one obtains still a decrease of 19% of the errors.

Finally, this new model can be easily applied to a multi dof robot, using (30) for each joint *j*.

This model is important for example in teleoperation, where the robots work at reduced velocity and can carry payloads or perform tasks with the effector subjected to external forces.

VI. Conclusion

This paper has presented a new dry friction model, with load- and velocity-dependency, and its identification method. The inverse dynamic model and the identification of its parameters have been successfully validated on a rotational joint of an industrial robot. As a result, one observes a significant improvement comparing to the usual model, for joints with large load variations, and especially at low velocity. Robots carrying important masses or with large inertial or gravity variations are concerned. In addition, this technique can be applied to multi dof robots.

Future works concern the application of this model to the multi dof robot and for different types of transmission. Then, the model will be used for torques monitoring and collision detection.

Acknowledgment

The authors thank the AREVA society [24] for the availability of the Stäubli RX130L robot.

References

[1] C. G. Atkeson, C. H. An, and J. M. Hollerbach, “Estimation of Inertial Parameters of Manipulator Loads and Links”, in *Int. J. of Robotics Research*, vol. 5(3), 1986, pp. 101-119.

[2] J. Swevers, C. Ganseman, D. B. Tückel, J. D. de Schutter, and H. Van Brussel, “Optimal Robot excitation and Identification”, *IEEE Trans. on Robotics and Automation*, vol. 13(5), 1997, pp. 730-740.

[3] P. K. Khosla and T. Kanade, “Parameter Identification of Robot Dynamics”, in *Proc. 24th IEEE Conf. on Decision Control*, Fort-Lauderdale, December 1985.

[4] M. Prüfer, C. Schmidt, and F. Wahl, “Identification of Robot Dynamics with Differential and Integral Models: A Comparison”, in *Proc. 1994 IEEE Int. Conf. on Robotics and Automation*, San Diego, California, USA, May 1994, pp. 340-345.

[5] B. Raucent, G. Bastin, G. Campion, J. C. Samin, and P. Y. Willems, “Identification of Barycentric Parameters of Robotic Manipulators from External Measurements”, *Automatica*, vol. 28(5), 1992, pp. 1011-1016.

[6] M. Gautier, “Identification of robot dynamics”, in *Proc. IFAC Symp. On Theory of Robots*, Vienna, Austria, December 1986, pp. 351-356.

[7] M. Gautier, “Dynamic identification of robots with power model”, in *Proc. IEEE Int. Conf. on Robotics and Automation*, Albuquerque, 1997, pp. 1922-1927.

[8] M. Gautier and P. H. Poignet, “Extended Kalman filtering and weighted least squares dynamic identification of robot”, *Control Engineering Practice*, 2001.

[9] W. Khalil, M. Gautier, and P. Lemoine, “Identification of the payload inertial parameters of industrial manipulators”, *IEEE Int. Conf. on Robotics and Automation*, Roma, Italia, April 2007, pp. 4943-4948.

[10] H. Kawasaki and K. Nishimura, “Terminal-link parameter estimation and trajectory control of robotic manipulators”, *IEEE J. of Robotics and Automation*, vol. RA-4(5), pp. 485-490, 1988.

[11] W. Khalil and E. Dombre, *Modeling, identification and control of robots*. Hermes Penton, London, 2002.

[12] M. Gautier and W. Khalil, “Direct calculation of minimum set of inertial parameters of serial robots”, *IEEE Trans. on Robotics and Automation*, vol. RA-6(3), 1990, pp. 368-373.

[13] M. Gautier, “Numerical calculation of the base inertial parameters”, *J. of Robotic Systems*, vol. 8(4), August 1991, pp. 485-506.

[14] P. P. Restrepo and M. Gautier, “Calibration of drive chain of robot joints”, in *Proc. 4th IEEE Conf. on Control Applications*, Albany, 1995, pp. 526-531.

[15] A. Gogoussis and M. Donath, “Coulomb friction effects on the dynamics of bearings and transmissions in precision robot mechanisms”, in *Proc. IEEE Int. Conf. on Robotics and Automation*, Philadelphia, Pennsylvania, April 1988, vol. 3, pp. 1440-1446.

[16] M. E. Dohring, E. Lee, and W. S. Newman, “A load-dependent transmission friction model: theory and experiments”, in *Proc. IEEE Int. Conf. on Robotics and Automation*, Atlanta, Georgia, May 1993, vol. 3, pp. 430-436.

[17] C. Pelchen, C. Schweiger, and M. Otter, “Modeling and simulation the efficiency of gearboxes and of planetary gearboxes”, in *Proc. 2nd International Modelica Conference*, Oberpfaffenhofen, Germany, March 2002, pp. 257-266.

[18] N. Chaillet, G. Abba, and E. Ostertag, “Double dynamic modelling and computed-torque control of a biped robot”, in *Proc. IEEE/RSJ/GI Int. Conf. on Intelligent Robots and Systems, 'Advanced Robotics Systems and the Real Word'*, Munich, Germany, September 1994, vol. 2, pp. 1149-1155.

[19] P. Garrec, J.-P. Friconneau, Y. Measson, and Y. Perrot, “ABLE, an Innovative Transparent Exoskeleton for the Upper-Limb”, *IEEE Int. Conf. on Intelligent Robots and Systems*, Nice, France, September 2008, pp. 1483-1488.

[20] H. Olsson, K. J. Aström, C. Canudas de Wit, M. Gäfvert and P. Lischinsky, “Friction Models and Friction Compensation”, in *European Journal of Control*, vol 4(3), 1998, pp. 176-195.

[21] B. Armstrong-Hélouvry, *Control of machines with friction*. Springer, Boston, 1991.

[22] J. Swevers, F. Al-Bender, C. G. Ganseman, and T. Prajogo, “An Integrated Friction Model Structure with Improved Presliding Behavior for Accurate Friction Compensation”, *IEEE Trans. on Automatic Control*, vol. 45(4), 2000, pp. 675-686.

[23] Mathworks website, http://www.mathworks.com/

[24] AREVA website, http://www.areva.com/

[25] Stäubli website, http://www.staubli.com/